

# Optical and EPR Detection of a Triplet Ground State Phenyl Nitrenium Ion

Yunfan Qiu<sup>†</sup>, Lili Du<sup>‡</sup>, Sarah Cady<sup>†</sup>, David Lee Phillips<sup>\*‡</sup>, Arthur H. Winter<sup>\*†</sup>

<sup>†</sup> Department of Chemistry, Iowa State University, 2101d Hach Hall, Ames, Iowa 50011, United States

<sup>‡</sup> Department of Chemistry, University of Hong Kong, Pokfulam Road, Hong Kong, S.A.R., P. R. China

## ABSTRACT

Nitrenium ions are important reactive intermediates participating in synthetic chemistry and biological processes. Phenyl nitrenium ions (Ph-NH<sup>+</sup>) typically have closed-shell singlet ground states with large singlet–triplet energy gaps, while little is known of triplet nitrenium ions regarding their reactivity, lifetimes, spectroscopic signatures, and electronic configurations. In this work, *m*-pyrrolidinyl-phenyl hydrazine hydrochloride (**1**) is synthesized as the photoprecursor to photochemically generate the corresponding *m*-pyrrolidinyl-phenyl nitrenium ion (**2**), which is computed to adopt a  $\pi,\pi^*$  triplet ground state. A combination of femtosecond (fs-) and nanosecond (ns-) transient absorption (TA) spectroscopy, cryogenic continuous-wave electronic paramagnetic resonance (CW-EPR) spectroscopy, computational analysis, and photoproduct studies, elucidated the complete photolysis pathway of this photoprecursor and offers the first direct experimental detection of a ground state triplet nitrenium ion. Upon photoexcitation, **1** is optically pumped to singlet excited states, followed by internal conversion (IC) to S<sub>1</sub> on the sub-picosecond timescale, where bond heterolysis occurs and the NH<sub>3</sub> leaving group is extruded in 1.8 ps, generating a vibrationally-hot, spin-conserving closed-shell singlet phenyl nitrenium ion (<sup>1</sup>**2**) that undergoes vibrational cooling in 19 ps. Subsequent intersystem crossing (ISC) takes place in 534 ps, yielding the ground state triplet phenyl nitrenium ion (<sup>3</sup>**2**), with a lifetime of 0.8  $\mu$ s. Unlike electrophilic singlet phenyl nitrenium ions, this triplet phenyl nitrenium reacts through sequential H atom abstractions, resulting in the eventual formation of the reduced *m*-pyrrolidinyl-aniline as the predominant stable photoproduct. Supporting the triplet ground state, continuous irradiation of **1** in a glassy matrix at 80 K forms a paramagnetic species consistent with the triplet nitrenium ion by cryogenic CW-EPR spectroscopy.

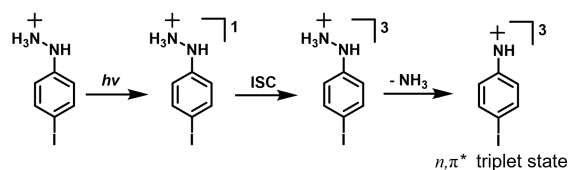
## INTRODUCTION

Nitrenium ions are reactive intermediates with the general formula of RNR<sup>+</sup>, which are isoelectronic with carbenes but have a positive charge on the hypovalent nitrogen atom.<sup>1,2</sup> Biochemically, nitrenium ions are postulated as the ultimate carcinogen from metabolic oxidation of aromatic amines<sup>3</sup> found in charred meats and dyes<sup>4</sup>, etc. They can also be generated chemically or photochemically as reactive synthetic intermediates. In particular, aryl nitrenium ions, denoted as Ar-NR<sup>+</sup>, have been extensively studied driven by their presence in synthetic chemistry<sup>5</sup> and biological processes as suspected carcinogens capable of causing DNA damage and modification.<sup>6-10</sup>

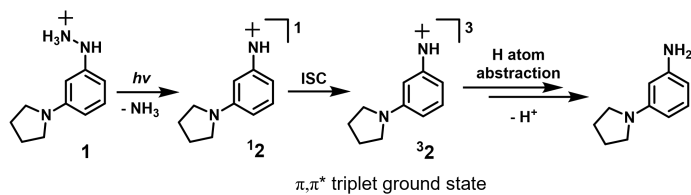
1 Generally, most aryl nitrenium ions (Ar-NH<sup>+</sup>) have closed-shell singlet ground states with large singlet–  
 2 triplet gaps resulting from a strong break in the degeneracy of the *p* orbitals on the formal nitrenium  
 3 center, whose vacant *p* orbital receives the electron density contribution from the filled  $\pi$  orbital of the  
 4 aromatic ring. For instance, the parent phenyl nitrenium ion is predicted to be a singlet ground state  
 5 species with  $\Delta E_{ST}$  of  $-20$  kcal/mol to an  $n,\pi^*$  triplet state.<sup>11</sup> In contrast to the many studies of singlet  
 6 aryl nitrenium ions, there remains a dearth of knowledge regarding the reactivity, lifetimes,  
 7 spectroscopic signatures, and electronic configurations of triplet phenyl nitrenium ions because the  
 8 triplet state is usually not the energetically preferred ground state. Experimental exploration of an N-  
 9 tert-butyl aryl nitrenium ion, conducted by Falvey et al., inferred the intermediacy of a triplet species  
 10 based on indirect product studies using external triplet photo-sensitizers and H atom donors.<sup>12, 13</sup> Only  
 11 recently was the first triplet nitrenium ion observed, the  $n,\pi^*$  triplet *p*-iodo-phenyl nitrenium ion, as  
 12 depicted in Figure 1. This system harnessed the heavy atom effect and rapid intersystem crossing (ISC)  
 13 by employing an iodine atom to generate an  $n,\pi^*$  triplet nitrenium ion in its excited triplet state. In that  
 14 case, the excited triplet undergoes rapid ISC into the ground singlet state, preventing a study of its  
 15 reactivity, but providing a first glimpse at an elusive triplet phenyl nitrenium ion.<sup>14</sup>

16 Nevertheless, to date, a direct optical or EPR detection of a triplet ground state phenyl nitrenium ion  
 17 remains unattained despite several computational studies that have predicted the existence of triplet  
 18 ground state aryl nitrenium ions.<sup>15-18</sup> A computational study investigating the impact of *meta*  
 19 substitution on the  $\Delta E_{ST}$  (singlet-triplet energy gap) of phenyl nitrenium ions revealed that substituting  
 20 the *meta* positions of the benzylic cations with strong  $\pi$  donors (e.g., NH<sub>2</sub>) stabilizes an *m*-xylylene-like  
 21  $\pi,\pi^*$  triplet state in preference to the singlet state.<sup>16</sup> This *meta*-effect has recently been validated  
 22 experimentally, where phenyl oxenium ion exhibits a triplet ground state when appending a  $\pi$  donor on  
 23 the *meta* position.<sup>19</sup> We anticipated that such an effect should be applicable to phenyl nitrenium ions  
 24 also.

**Prior work:**



**This work:**



25

26 **Figure 1.** (Top) First detection of an excited triplet  $n,\pi^*$  state of a nitrenium ion. (Bottom) This work,  
 27 providing the first direct detection of a ground state triplet phenyl nitrenium ion.

1

2 In this study, we synthesized *m*-pyrrolidinyl-phenyl hydrazine hydrochloride (**1**) as the photoprecursor  
3 for the corresponding *m*-pyrrolidinyl-phenyl nitrenium ion (**2**), which consists of a robust *meta*  $\pi$  donor  
4 (i.e. pyrrolidine). Employing femtosecond (fs-) and nanosecond (ns-) transient absorption (TA)  
5 spectroscopy, cryogenic continuous-wave electronic paramagnetic resonance (CW-EPR) spectroscopy,  
6 computational analysis, and photoproduct studies, we reveal that nitrenium ion **2** is a  $\pi, \pi^*$  triplet ground  
7 state species with a lifetime of 0.82  $\mu$ s. Both optical and matrix EPR spectra affirm the discrete existence  
8 of the triplet species and photoproduct studies highlight its radical-like reactivity, which is exemplified  
9 by the predominant formation of the stable photoproduct, reduced *m*-pyrrolidinyl-aniline, resulting from  
10 sequential H atom abstractions.

## 11 EXPERIMENTAL METHODS

12 **Synthesis and Characterization.** Detailed synthetic procedures and characterizations of the  
13 photoprecursor **1** are given in the Supporting Information. Spectroscopic grade acetonitrile (MeCN)  
14 and deionized water were used to prepare the sample solutions for the time-resolved spectroscopy  
15 experiments. All the mixed solvent ratios are of volume ratios unless indicated otherwise.

16 **Fs- and ns-TA spectroscopy.** The experimental setups and method for transient absorption  
17 experiments have been described in our previous studies.<sup>20, 21</sup> The fs-TA experiments were conducted  
18 on a commercialized Helios pump-probe system (Ultrafast System) with the femtosecond laser beam  
19 from the regenerative amplified Ti:sapphire laser system (Spectra Physics, Spitfire Pro). The laser light  
20 (120 fs, 800 nm) was then split into two beams with one using as the pump beam and one as the probe  
21 beam. For the present experiments, the wavelength of the pump beam was set as 267 nm (the third  
22 harmonic of the fundamental 800 nm), while the probe beam passed through a CaF<sub>2</sub> crystal and  
23 generated a white-light continuum (330–650 nm). After the solution was photoexcited by the pump  
24 light, the time-delayed probe beam (controlled by the optical delay rail with a maximum temporal delay  
25 at 3.3 ns) was passed through the photoexcited solution and the TA signals were then collected by the  
26 detector. A reference probe beam was also used to obtain a better signal-to-noise ratio. The 80 mL  
27 sample solutions were prepared with absorbance around 1 at 267 nm and circulated in a 2 mm path-  
28 length quartz cuvette. The ns-TA experiments were performed on a LP920 laser flash spectrometer by  
29 Edinburgh Instruments Ltd. Briefly, the continuous probe light ranged from 280 to 800 nm was  
30 produced by a 450 W ozone free Xe arc lamp, and the 266 nm pump beam was obtained from the fourth  
31 harmonic output of an Nd:YAG laser. The 80 mL sample solutions with an absorption of around 1 at  
32 266 nm were prepared in a flowing 1 cm path-length quartz cuvette. The transmitted signals were  
33 collected by a photomultiplier detector (for kinetics mode) and an array detector (for spectral mode).  
34 The instrument response function (irf) of ns-TA is 20 ns.

1 **Continuous-Wave (CW) Electron Paramagnetic Resonance (EPR) Spectroscopy.** EPR  
2 measurements at X-band were made on a Bruker ELEXSYS E580 FT-EPR spectrometer incorporated  
3 with a temperature control cryostat capable of achieving liquid nitrogen temperatures (80 K) and  
4 equipped with a UV-emitting mercury light source channeled into the resonator cavity using a fiber  
5 optic cable. **1** is dissolved in anhydrous EtOH at a concentration of 1 mg/mL. The solution is pre-frozen  
6 to create a glassy matrix to maximize light penetration before being inserted into the resonator. Data  
7 collection was performed at various durations of light irradiation. The data were processed and  
8 simulated in MATLAB utilizing functions from the EasySpin software package.<sup>22</sup>

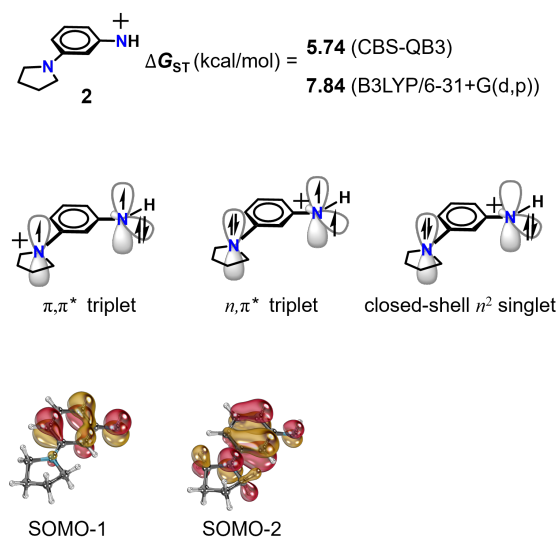
9 **Computational Methods.** The singlet–triplet gap ( $\Delta E_{ST}$ ) of **2** was estimated using density functional  
10 theory (B3LYP/6-31G+(d,p)) and the accurate compound method CBS-QB3. The TD-DFT  
11 methodology (TD-B3LYP/6-31G+(d,p)). was performed to predict the UV–vis absorption spectra of  
12 the transient species generated from the photolysis of the photoprecursor. Polarizable continuum model  
13 (PCM) was also applied when computing the absorption spectra. No imaginary frequency modes were  
14 observed at the stationary states of the optimized structures. All of the calculations were performed  
15 using the Gaussian 09 program.<sup>23</sup>

16 **Photoproduct studies.** Product studies were conducted using 2.5 mg of precursor **1** dissolved in 1 mL  
17 of solvent in a quartz NMR tube. The sample was then subjected to irradiation with 254 nm UV light  
18 emitted from a mercury vapor lamp for desired time intervals in a Rayonet photoreactor. Once the  
19 photolysis was complete and confirmed by the disappearance of initial <sup>1</sup>H NMR peaks, the sample was  
20 submitted to LC-MS using Agilent QTOF 6540 with an ESI ionization method for further product  
21 analysis and confirmation.

## 22 **RESULTS AND DISCUSSION**

23 **Theoretical Prediction of the Ground State Electronic Configuration for 2.** As shown in Figure 2.  
24 the  $\Delta E_{ST}$  values for **2** were computed to be +5.7 and +7.8 kcal/mol at the level of CBS-QB3 and  
25 B3LYP/6-31+G(d,p), respectively. A positive value indicates a triplet ground state. These relatively  
26 large  $\Delta E_{ST}$  values make a clear prediction that **2** adopts a triplet ground state. Visualization of the two  
27 singly occupied molecular orbitals (SOMOs) in the triplet manifold reveals that the triplet ground state  
28 is associated with non-disjoint  $\pi, \pi^*$  SOMOs, in contrast to the previously observed  $n, \pi^*$  triplet state  
29 (Figure 1), which leads to large exchange energies favoring the triplet state.<sup>24</sup> Moreover, both SOMOs  
30 exhibit delocalized  $\pi$  characters spanning across the phenyl ring and the  $p$  orbital of the nitrogen center,  
31 indicative of a  $\pi, \pi^*$  electronic configuration. Figure 2 also illustrates simple schematic models for the  
32 lowest electronic states of *meta*-donor-substituted phenyl nitrenium ions. The lowest singlet state is  
33 designated “ $n^2$ ”, referring to the occupancy of the HOMO. The lowest triplet state typical of non-*meta*  
34 donor aryl nitrenium ions is designated as “ $n, \pi^*$ ”. This state is derived from promotion of an electron  
35 from the  $n$  orbital on the nitrenium center to a  $\pi^*$  orbital, which results from the mixing of the

1 nonbonding orbital on the nitrogen atom and the  $\pi^*$  orbitals of the phenyl ring. Finally, the lowest triplet  
 2 state of the *meta*  $\pi$ -donors is designated as “ $\pi,\pi^*$ ”, indicating that this state is derived from promotion  
 3 of an electron on a substituent nonbonding orbital of  $\pi$ -symmetry to the  $\pi^*$  level. This can be visualized  
 4 by starting with the aryl nitrenium ion's singlet state, and then transferring an electron from a  
 5 nonbonding orbital on the donor substituent(s) to the out-of-plane nonbonding orbital on the nitrenium  
 6 ion center. This would create a species that would have aminyl radical character at the initial nitrenium  
 7 ion center and a cation radical site on the *meta* substituent(s).

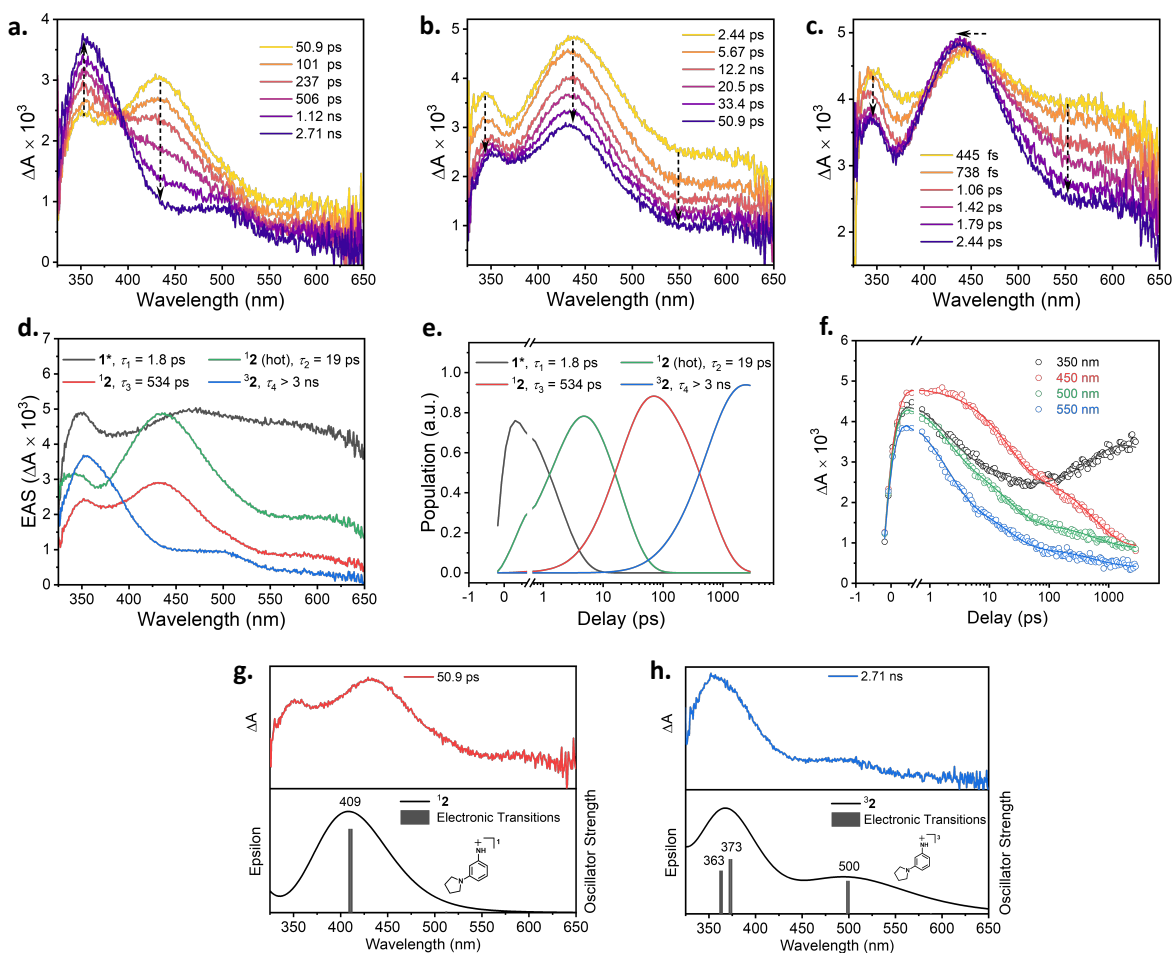


8

9 **Figure 2.** (top) Calculated  $\Delta E_{ST}$  for **2** using different methods. (middle) Possible schematic electronic  
 10 configurations for **2**. Computations suggest the ground state configuration is  $\pi,\pi^*$  triplet and the lowest  
 11 energy singlet state is the closed-shell configuration. (bottom) Visualized Kohn–Sham molecular  
 12 orbitals for the two SOMO orbitals show the  $\pi,\pi^*$  nature of the triplet state of  $^3\mathbf{2}$ .

13 **Femtosecond Transient Absorption (fs-TA) Study of 1.** Photolysis of **1** was examined using fs-TA  
 14 experiments performed in 1.4 %  $\text{H}_2\text{O}$  in MeCN. The addition of water was employed to aid in the  
 15 dissolution of the ionic photoprecursors. Once irradiated using 267 nm pump, within 445 fs, **1** was  
 16 photoexcited to its higher singlet excited  $S_n$ . Following Kasha's rule<sup>25</sup>, it subsequently underwent  
 17 internal conversion to  $S_1$ , whose absorption spectra features a sharp peak at 348 nm and a broad band  
 18 extending from 390 nm to 650 nm, centered at 465 nm. Photoheterolysis then occurs spontaneously, as  
 19 shown in Figure 3a, evidenced by two key observations: 1) a reduction in optical intensity of the initial  
 20 sharp peak at 348 nm, accompanied by a slight redshift, and 2) significant narrowing and blue-shifting  
 21 of the previously broad absorption band, now centered at 430 nm. Over the course of approximately 50  
 22 ps, as illustrated in Figure 3b, the spectroscopic characteristics of this singlet state phenyl nitrenium ion  
 23 retain but its optical intensity has a noticeable decay. This process is attributed to vibrational cooling  
 24 wherein the initially hot-born phenyl nitrenium ion dissipates excess energy to the solvent, a  
 25 phenomenon that has been observed in the prior work.<sup>19</sup> In the subsequent photochemical process, as  
 26 displayed in Figure 3c, the prominent peak at 430 nm associated with the singlet phenyl nitrenium ion

1 gradually diminishes in intensity. Concomitantly, a new peak emerges at 355 nm, along with the  
 2 appearance of a broad peak at 506 nm. This process exhibits an isosbestic point at approximately 393  
 3 nm, indicating a clean transformation between a precursor species and a product species. This result  
 4 strongly suggests that the singlet nitrenium ion undergoes a transformation, either through a chemical  
 5 reaction or a change into a distinct electronic configuration.



6

7 **Figure 3.** Shown are the fs-TA spectra acquired after 267 nm excitation of the precursor **1** (a) from 445  
 8 fs to 2.44 ps, (b) from 2.44 ps to 50.9 ps, (c) from 50.9 ps to 2.71 ns. (d) EAS according to the sequential  
 9 kinetic models. (e) Time evolution of the populations of the kinetic species obtained from the global  
 10 fitting analysis. Color of the fitting trace is consistent with the EAS spectra. (f) Kinetics fits to the raw  
 11 data at the indicated wavelengths using the sequential kinetic model. (g) Comparison between (top, red)  
 12 the experimental data obtained at 50.9 ps and (bottom) the calculated UV-vis spectra of the  $^1\mathbf{2}$  (closed-  
 13 shell  $n^2$  singlet). (h) Comparison between (top, blue) the experimental data obtained at 2.71 ns and  
 14 (bottom) the calculated UV-vis spectra of the  $^3\mathbf{2}$  ( $\pi,\pi^*$  triplet).

15

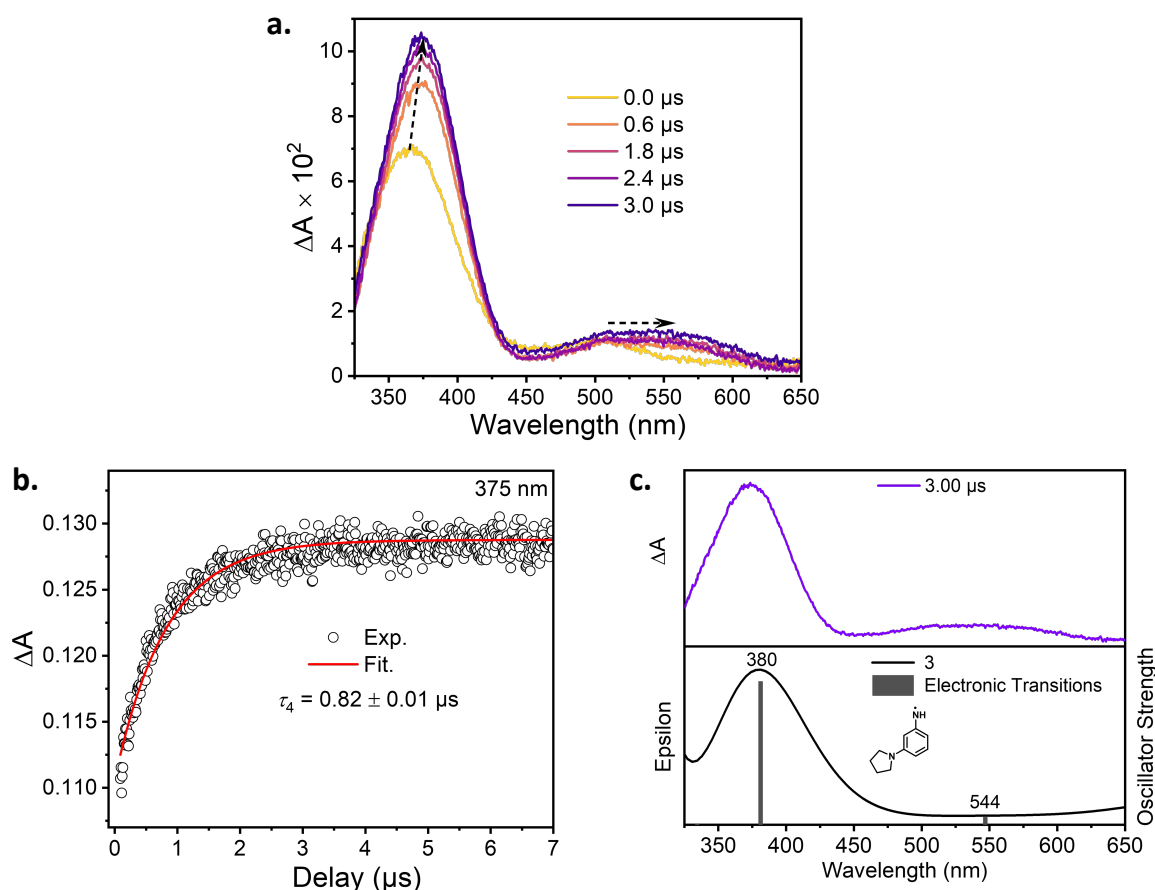
16 Global analysis yields four evolution associated difference spectra (EAS) in Figure 3d, corresponding  
 17 to four distinct kinetic species, whose lifetimes are resolved through time evolution of species  
 18 population, shown in Figure 3e, as 1.8 ps (black), 19 ps (green), 534 ps (red) and  $> 3$  ns (blue),  
 19 respectively. Notably, the decay time constant of the last species (blue) exceeds the timescale of our fs-

1 TA instrument and was further examined using ns-TA, discussed later. The kinetics fit, shown in Figure  
2 3f, exhibits excellent agreement with the experimental data, confirming that the proposed sequential  
3 kinetic model effectively represents the experiment data. Assignments of the kinetic species are  
4 performed through a comparative analysis, utilizing existing spectroscopic features of singlet nitrenium  
5 ions and computed UV-vis spectra that are shown in Figure 3g and 3h. Though the theoretically  
6 predicted UV-vis spectrum of  $^1\mathbf{2}$  exhibits a blue shift, it's important to note that numerous previously  
7 reported spectroscopic observations of phenyl nitrenium ions in their singlet state consistently show  
8 similar absorption features at approximately 450 nm.<sup>10, 26, 27</sup> This observed spectroscopic shift, when  
9 compared to the computational prediction, can be attributed to the formation of water complexes.<sup>19</sup>  
10 Moreover, the homolysis product, aminyl radical can also be ruled out because the short lifetime ( $\tau_3 =$   
11 534 ps) of this species. Therefore, we assign the species after the photoexcited photo precursor to  $^1\mathbf{2}$   
12 formed from an excited state photoheterolysis process.

13 It is noteworthy that the lifetime of this singlet nitrenium ion is still considerably shorter than most  
14 detected phenyl nitrenium ions, which typically have lifetimes exceeding hundreds of nanoseconds to  
15 microseconds by reacting with surrounding nucleophiles due to its electron-deficient nature and  
16 associated resonant structures (Scheme S2, Supporting Information).<sup>1, 2</sup> A difference is that with this  
17 nitrenium ion, the ground state of this phenyl nitrenium ion is calculated to be the triplet state. Although  
18 the nitrenium ion is initially generated in a singlet spin state due to the spin-conserving nature of the  
19 photoheterolysis step, it relaxes to its ground state, a  $\pi, \pi^*$  triplet through ISC. The relatively small  
20 computed singlet-triplet energy gap further facilitates this transition from the singlet state to the triplet  
21 spin multiplicity. Consequently, we attribute the transformation depicted in Figure 3c to the ISC process.  
22 Additionally, the computed UV-vis spectrum presented in Figure 3g for the  $^3\mathbf{2}$  aligns well with the  
23 experimental spectrum extracted at 2.71 ns.

24 **Nanosecond Transient Absorption (ns-TA) Study of 1.** To provide the integrated spectra of the later  
25 species beyond 3 ns, ns-TA was employed to study the reaction pathways of precursor **1** in 1.4 % H<sub>2</sub>O  
26 in MeCN after irradiation. Figure 4a shows that the absorption band at 355 nm, associated with  $^3\mathbf{2}$ ,  
27 continues to increase in intensity and slightly red-shift to 375 nm. Simultaneously, the broad band  
28 centered at 506 nm undergoes a significant red shift to 550 nm, accompanied by a broader feature.  
29 These changes unambiguously demonstrate a new transient species has formed. The temporal  
30 dependences of the transient absorption intensity at 375 nm can be mathematically fitted by a  
31 monoexponential function, as displayed in Figure 4b, which gives a time constant of  $\tau_4 = 0.82 \mu\text{s}$ ,  
32 representing the lifetime of  $^3\mathbf{2}$  that complements the fs-TA analysis. Importantly, the optical spectrum  
33 of the generated species closely matches the computed UV-vis spectrum of the *m*-pyrrolidinyl-phenyl  
34 aminyl radical (**3**). This radical species is expected to derive from  $^3\mathbf{2}$  through a process involving H  
35 atom abstraction and subsequent deprotonation. Such radical reactivity of  $^3\mathbf{2}$  is anticipated as triplet  
36 state can be conceptually interpreted as comprising two radical centers with a certain degree of

1 exchanging or dipolar coupling strength. The assignment of **3** is further corroborated in the  
 2 photoproduct studies discussed later in the context, where the primary photoproduct is the reduced *m*-  
 3 pyrrolidiny-aniline. **3** has a long lifetime of  $\tau_5 = 487 \mu\text{s}$  in solutions before it produces the ultimate  
 4 photoproduct. (Figure S8, Supporting Information).

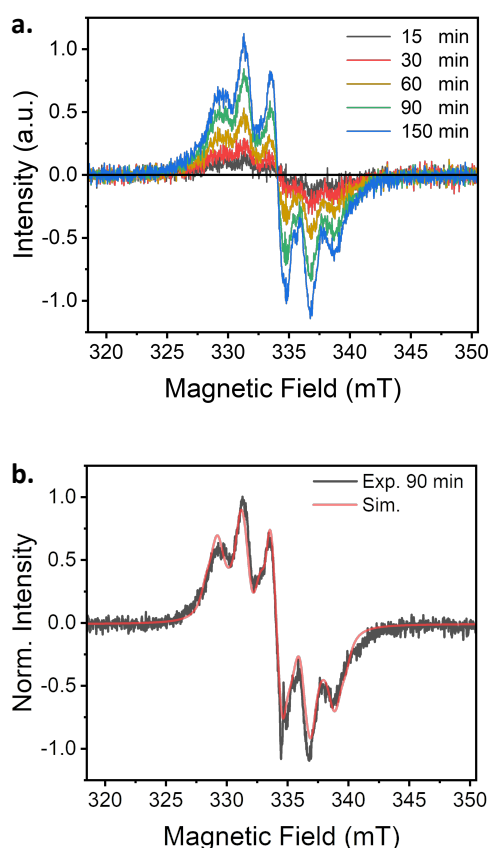


5  
 6 **Figure 4.** (a) Shown are ns-TA spectra acquired from 0  $\mu\text{s}$  (irf =20 ns) – 440  $\mu\text{s}$ . (b) Temporal  
 7 dependences of the transient absorption intensity of initial compound at 375 nm in long time region.  
 8 Solid red line indicates fittings using a monoexponential function. (c) Comparison of (top, purple) the  
 9 experimental data obtained at 3.00  $\mu\text{s}$  and (bottom) the calculated UV-vis spectra of the **3** (aminyl  
 10 radical).

11  
 12 **Cryogenic CW-EPR Study of 1.** Additional evidence supporting the ground state of **2** as a triplet state  
 13 comes from low-temperature matrix isolation EPR experiments. At cryogenic temperatures, most non-  
 14 tunneling reactions are effectively suppressed due to the lack of activation energy. Moreover, the frozen  
 15 matrix constrains molecular motions, further preventing chemical reactions. Furthermore, operating at  
 16 80 K, which corresponds to thermal energy of only 0.16 kcal/mol, essentially no thermal population of  
 17 an excited triplet state would be possible outside of having virtually degenerate singlet and triplet  
 18 energies. To probe the triplet signal of <sup>3</sup>**2**, a photolysis study of **1** within a low-temperature EtOH glassy  
 19 matrix at 80 K was conducted. As shown in Figure 5a, continuous light irradiation leads to the



1 progressive growth of the paramagnetic species, indicating ongoing photolysis. The resulting species  
2 are effectively locked within the rigid solid environment, enabling an exploration of their spin states.  
3 The signal, which exceeds 20 mT in the EPR spectra, strongly suggests the formation of a triplet  
4 diradical species rather than a  $S=1/2$  species. However, a monoradical impurity is also present, possibly  
5 arising from a competitive homolysis pathway in the solid state or H-atom transfer from nearby on the  
6 pyrrolidinyll group. The convoluted spectra can be simulated by as a sum of contributions from both a  
7 triplet species and a mono-radical impurity (Figure S7, Supporting Information).



8

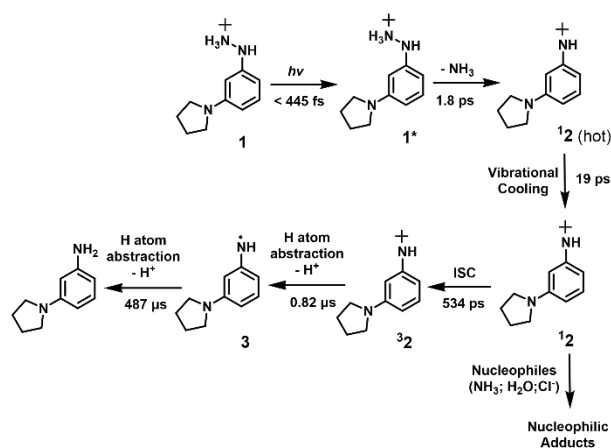
9 **Figure 5.** (a) Time resolved EPR spectra recorded under different durations of UV light irradiation. (b)  
10 The experimental EPR data collected after 90 minutes of irradiation (black), overlaid with the  
11 simulation (red). Detailed simulation parameters can be found in Supporting Information.

12

13 Figure 5b shows the spectrum collected at 90 minutes after UV, with the superimposed simulation  
14 demonstrating excellent agreement. Notably, the zero-field splitting (ZFS) tensors, characterized by the  
15  $|D|/hc$  parameter ( $0.0048 \text{ cm}^{-1}$ ) and  $|E|/hc$  parameter ( $0.0002 \text{ cm}^{-1}$ ), are even smaller than other triplet  
16 *meta*-xylylene-like diradical species that have small dipolar couplings and similar electronic  
17 structures.<sup>28-30</sup> However, the spectrum shape strongly resembles the spectrum of the triplet *m*-xylylene  
18 diradical, which has an analogous electronic structure but is an all-carbon species.<sup>28</sup> Nevertheless, the  
19 absence of a detectable forbidden transition of  $\Delta M_s = \pm 2$  is consistent with the very small  $|D|/$  value

1 and possibly exchange coupling is also contributing to the EPR spectra and giving diminished ZFS  
2 values.<sup>31, 32</sup>

3 **Photoproduct Study of 1 and Proposed Photolysis Pathway.** A triplet ground state of **2** is further  
4 supported by the photoproduct analysis, which was performed in 1.4 % H<sub>2</sub>O in MeCN or in H<sub>2</sub>O. <sup>1</sup>H  
5 NMR characterization was used to determine the completion of the photolysis and LC-MS was used to  
6 isolate photoproducts for further analysis and product confirmation. Figures S4-S6 in the Supporting  
7 Information show that the predominant product is the reduced *m*-pyrrolidinyl-aniline, suggesting the  
8 radical-like reactivity of the triplet nitrenium ion <sup>3</sup>**2**. Additionally, some nucleophilic adducts are  
9 observed, likely originating from reactions of the initially generated <sup>1</sup>**2** with the Cl counterion in the  
10 precursor or with water. As mentioned earlier, nucleophile adducts of a singlet phenyl nitrenium ion are  
11 typically expected due to the presence of resonant structures that create carbon cations on the phenyl  
12 aromatic ring (Scheme S2, Supporting Information). The reactivity of triplet phenyl nitrenium ions has  
13 received limited attention due to their infrequent occurrence in studies, but by drawing parallels with  
14 related reactive intermediates, such as carbenes and nitrenes, one might anticipate radical ion chemistry,  
15 including processes like H-atom abstraction. The formation of the reduced product resulting from the  
16 photolysis of **1** suggests that a triplet nitrenium ion could be involved, likely through sequential H-atom  
17 abstraction processes followed by proton loss, rather than nucleophilic trapping chemistry. The presence  
18 of nucleophile adducts is not surprising as they indicate the generation of the excited singlet species <sup>1</sup>**2**.  
19 Competing against the ISC conversion within 534 ps, nucleophilic addition acts as a concomitant singlet  
20 decay channel. Moreover, the H atom abstraction reactions that happen at the cationic radical and  
21 aminyl radical centers of <sup>3</sup>**2** have been extensively documented in the literature.<sup>33-35</sup>



23 **Scheme 1.** Proposed mechanistic pathway.  
24

25 Based on optical and EPR spectroscopic data, computational prediction, and photoproduct analysis, we  
26 map out the complete photophysics and photochemistry pathways of **1** (Scheme 1). In detail, the process  
27 begins with the excitation of precursor **1** to its excited state, leading to photo-heterolysis where the NH<sub>3</sub>

1 leaving group is ejected. This results in the formation of a vibrationally excited (hot) phenyl nitrenium  
2 ion in its singlet state. Subsequently, this species undergoes rapid vibrational cooling over 19 ps to  
3 produce <sup>1</sup>**2**. Due to the electrophilic nature of the singlet nitrenium ion, some of this species undergoes  
4 nucleophilic trapping reactions to generate nucleophilic adducts. Next, <sup>1</sup>**2** undergoes ISC, a critical step  
5 leading to the formation of the triplet ground state <sup>3</sup>**2**, which is directly observed through transient  
6 absorption (TA) and EPR spectroscopy. Over a duration of 0.82 μs, <sup>3</sup>**2** initiates the formation of the  
7 aminyl radical through H-atom abstraction on the cationic radical nitrogen center on the pyrrolidinyl ,  
8 ultimately yielding the major photoproduct, reduced *m*-pyrrolidinyl-aniline, detected in the  
9 photoproduct studies.

## 10 CONCLUSIONS

11 In conclusion, a new photoprecursor for the generation of the phenyl nitrenium ion, *m*-pyrrolidinyl-  
12 phenyl nitrenium ion (**2**), was investigated using time-resolved optical spectroscopic experiments (fs-  
13 TA, and ns-TA) and EPR measurements along with computational calculations and photochemical  
14 product studies. These experiments allow us to draw several conclusions. First, **2** has a π,π\* triplet  
15 ground state, in contrast to the excited *n*,π\* triplet phenyl nitrenium ion reported previously.<sup>14</sup> Its  
16 reactivity engages in H atom abstractions to yield a reduced product, which is rather similar to triplet  
17 carbenes. Furthermore, this π,π\* triplet ground state of this nitrenium ion is shorter-lived than typical  
18 closed-shell singlet state nitrenium ions, living for 0.8 μs and marking its high reactivity in solution.  
19 Future work will focus on the intriguing possibilities to use this photochemically generated triplet  
20 nitrenium ion for practical synthetical applications.

## 21 ASSOCIATED CONTENT

### 22 Supporting Information

23 The Supporting Information is available free of charge on the ACS Publications website at DOI:XXXX.  
24 Supporting information includes description of synthesis and characterizations, photolysis product  
25 studies, additional TA spectra, EPR simulations, and computational details.

## 26 AUTHOR INFORMATION

### 27 Corresponding Authors

28 David Lee Phillips - Department of Chemistry, University of Hong Kong, Pokfulam Road, Hong Kong,  
29 S.A.R., P. R. China. Email: phillips@hku.hk

30 Arthur H. Winter - Department of Chemistry, Iowa State University, Ames, Iowa 50010, United States;  
31 orcid.org/0000-0003-2421-5578. Email: winter@iastate.edu

### 32 Authors

1 Yunfan Qiu - Department of Chemistry, Iowa State University, Ames, Iowa 50010, United States; ;  
2 orcid.org/0000-0002-4666-1424.

3 Lili Du - School of Life Sciences, Jiangsu University, 212013, Zhenjiang, P.R. China; Department of  
4 Chemistry, The University of Hong Kong, Pokfulam Road, Hong Kong, P.R. China; orcid.org/0000-  
5 0002-9712-3925.

6 Sarah Cady - Department of Chemistry, Iowa State University, Ames, Iowa 50010, United States;  
7 orcid.org/0000-0002-8310-7422.

## 8 Notes

9 The authors declare no competing financial interest.

## 10 ACKNOWLEDGMENTS

11 A.H.W. thanks PRF 62317-ND4 and the National Science Foundation for supporting this work  
12 through CHE-2055335. DLP thanks support from the Hong Kong Research Grants Council (GRF  
13 17302419, GRF 17316922), The University of Hong Kong Development Fund 2013-2014 project  
14 “New Ultrafast Spectroscopy Experiments for Shared Facilities”, Major Program of Guangdong Basic  
15 and Applied Research (2019B030302009), Key-Area Research and Development Program of  
16 Guangdong Province (2020B0101370003) and URC Seed Funding for Strategic Interdisciplinary  
17 Research Scheme (SIRS) 2019/20.

## 18 REFERENCES

- 19 (1) Moss, R. A.; Platz, M.; Jones, M., Jr. *Reactive Intermediate Chemistry*; Wiley:Hoboken, N.J, 2004.  
20 (2) Falvey, D.; Falvey, D. E.; Gudmundsdottir, A. D. *Nitrene and Nitrenium Ions*; Wiley:Hoboken,  
21 New Jersey, 2013.  
22 (3) Radomski, J. L.; Brill, E. Bladder Cancer Induction by Aromatic Amines: Role of N-Hydroxy  
23 Metabolites. *Science* **1970**, *167* (3920), 992-993.  
24 (4) Knize, M. G.; Cunningham, P. L.; Griffin, E. A.; Jones, A. L.; Felton, J. S. Characterization of  
25 mutagenic activity in cooked-grain-food products. *Food and Chemical Toxicology* **1994**, *32* (1), 15-21.  
26 (5) Lux, F. Properties of electronically conductive polyaniline: a comparison between well-known  
27 literature data and some recent experimental findings. *Polymer* **1994**, *35* (14), 2915-2936.  
28 (6) Novak, M.; Kahley, M. J.; Eiger, E.; Helmick, J. S.; Peters, H. E. Reactivity and selectivity of  
29 nitrenium ions derived from ester derivatives of carcinogenic N-(4-biphenyl)hydroxylamine and the  
30 corresponding hydroxamic acid. *Journal of the American Chemical Society* **2002**, *115* (21), 9453-9460.  
31 (7) Suzuki, H.; Ninoseki, T.; Hayashi, A.; Hase, Y.; Matsui, T.; Naito, M.; Sugai, S. Comparison of  
32 stabilities of Nitrenium Ions and in vitro and in vivo Genotoxic Potential, between Four Aniline  
33 Derivatives. *Fundamental Toxicological Sciences* **2018**, *5* (1), 21-32.  
34 (8) Turesky, R. J.; Le Marchand, L. Metabolism and Biomarkers of Heterocyclic Aromatic Amines in  
35 Molecular Epidemiology Studies: Lessons Learned from Aromatic Amines. *Chemical Research in*  
36 *Toxicology* **2011**, *24* (8), 1169-1214.  
37 (9) Skipper, P. L.; Kim, M. Y.; Sun, H. L. P.; Wogan, G. N.; Tannenbaum, S. R. Monocyclic aromatic  
38 amines as potential human carcinogens: old is new again. *Carcinogenesis* **2009**, *31* (1), 50-58.  
39 (10) McClelland, R. A.; Ahmad, A.; Dicks, A. P.; Licence, V. E. Spectroscopic Characterization of the  
40 Initial C8 Intermediate in the Reaction of the 2-Fluorenylnitrenium Ion with 2'-Deoxyguanosine.  
41 *Journal of the American Chemical Society* **1999**, *121* (14), 3303-3310.  
42 (11) Cramer, C. J.; Dulles, F. J.; Falvey, D. E. Ab Initio Characterization of Phenylnitrenium and  
43 Phenylcarbene: Remarkably Different Properties for Isoelectronic Species. *Journal of the American*  
44 *Chemical Society* **2002**, *116* (21), 9787-9788.

- 1 (12) Anderson, G. B.; Yang, L. L. N.; Falvey, D. E. Photogenerated arylnitrenium ions:  
2 photoisomerization of the N-tert-butyl-3-methylanthranilium ion and spin-selective reactivity of the  
3 isomeric arylnitrenium ion. *Journal of the American Chemical Society* **1993**, *115* (16), 7254-7262.
- 4 (13) Srivastava, S.; Falvey, D. E. Reactions of a Triplet Arylnitrenium Ion: Laser Flash Photolysis and  
5 Product Studies of N-tert-Butyl(2-acetyl-4-nitrophenyl)nitrenium Ion. *Journal of the American*  
6 *Chemical Society* **1995**, *117* (41), 10186-10193.
- 7 (14) Du, L.; Wang, J.; Qiu, Y.; Liang, R.; Lu, P.; Chen, X.; Phillips, D. L.; Winter, A. H. Generation  
8 and direct observation of a triplet arylnitrenium ion. *Nature Communications* **2022**, *13* (1).
- 9 (15) Qiu, Y.; Winter, A. H. Anomalous Electronic Properties of Iodous Materials: Application to High-  
10 Spin Reactive Intermediates and Conjugated Polymers. *The Journal of Organic Chemistry* **2020**, *85* (6),  
11 4145-4152.
- 12 (16) Winter, A. H.; Falvey, D. E.; Cramer, C. J. Effect of meta Electron-Donating Groups on the  
13 Electronic Structure of Substituted Phenyl Nitrenium Ions. *Journal of the American Chemical Society*  
14 **2004**, *126* (31), 9661-9668.
- 15 (17) Qiu, Y.; Fischer, L. J.; Dutton, A. S.; Winter, A. H. Aryl Nitrenium and Oxenium Ions with Unusual  
16 High-Spin  $\pi, \pi^*$  Ground States: Exploiting (Anti)Aromaticity. *The Journal of Organic Chemistry* **2017**,  
17 *82* (24), 13550-13556.
- 18 (18) Sullivan, M. B.; Brown, K.; Cramer, C. J.; Truhlar, D. G. Quantum Chemical Analysis of para-  
19 Substitution Effects on the Electronic Structure of Phenylnitrenium Ions in the Gas Phase and Aqueous  
20 Solution. *Journal of the American Chemical Society* **1998**, *120* (45), 11778-11783.
- 21 (19) Li, M.-D.; Albright, T. R.; Hanway, P. J.; Liu, M.; Lan, X.; Li, S.; Peterson, J.; Winter, A. H.;  
22 Phillips, D. L. Direct Spectroscopic Detection and EPR Investigation of a Ground State Triplet Phenyl  
23 Oxenium Ion. *Journal of the American Chemical Society* **2015**, *137* (32), 10391-10398.
- 24 (20) Du, L.; Li, M.-D.; Zhang, Y.; Xue, J.; Zhang, X.; Zhu, R.; Cheng, S. C.; Li, X.; Phillips, D. L.  
25 Photoconversion of  $\beta$ -Lapachone to  $\alpha$ -Lapachone via a Protonation-Assisted Singlet Excited State  
26 Pathway in Aqueous Solution: A Time-Resolved Spectroscopic Study. *The Journal of Organic*  
27 *Chemistry* **2015**, *80* (15), 7340-7350.
- 28 (21) Li, M.-D.; Ma, J.; Su, T.; Liu, M.; Yu, L.; Phillips, D. L. Direct Observation of Triplet State  
29 Mediated Decarboxylation of the Neutral and Anion Forms of Ketoprofen in Water-Rich, Acidic, and  
30 PBS Solutions. *The Journal of Physical Chemistry B* **2012**, *116* (20), 5882-5887.
- 31 (22) Stoll, S.; Schweiger, A. EasySpin, a comprehensive software package for spectral simulation and  
32 analysis in EPR. *Journal of Magnetic Resonance* **2006**, *178* (1), 42-55.
- 33 (23) M. J. Frisch, G. W. T., H. B. Schlegel, G. E. Scuseria, M. A. Robb, J. R. Cheeseman, G. Scalmani,  
34 V. Barone, G. A. Petersson, H. Nakatsuji, X. Li, M. Caricato, A. Marenich, J. Bloino, B. G. Janesko, R.  
35 Gomperts, B. Mennucci, H. P. Hratchian, J. V. Ortiz, A. F. Izmaylov, J. L. Sonnenberg, D. Williams-  
36 Young, F. Ding, F. Lipparini, F. Egidi, J. Goings, B. Peng, A. Petrone, T. Henderson, D. Ranasinghe,  
37 V. G. Zakrzewski, J. Gao, N. Rega, G. Zheng, W. Liang, M. Hada, M. Ehara, K. Toyota, R. Fukuda, J.  
38 Hasegawa, M. Ishida, T. Nakajima, Y. Honda, O. Kitao, H. Nakai, T. Vreven, K. Throssell, J. A.  
39 Montgomery, Jr., J. E. Peralta, F. Ogliaro, M. Bearpark, J. J. Heyd, E. Brothers, K. N. Kudin, V. N.  
40 Staroverov, T. Keith, R. Kobayashi, J. Normand, K. Raghavachari, A. Rendell, J. C. Burant, S. S.  
41 Iyengar, J. Tomasi, M. Cossi, J. M. Millam, M. Klene, C. Adamo, R. Cammi, J. W. Ochterski, R. L.  
42 Martin, K. Morokuma, O. Farkas, J. B. Foresman, and D. J. Fox. Gaussian, Inc., Wallingford CT, 2016.
- 43 (24) Borden, W. T.; Iwamura, H.; Berson, J. A. Violations of Hund's Rule in Non-Kekule Hydrocarbons:  
44 Theoretical Prediction and Experimental Verification. *Accounts of Chemical Research* **2002**, *27* (4),  
45 109-116.
- 46 (25) Kasha, M. Characterization of electronic transitions in complex molecules. *Discussions of the*  
47 *Faraday Society* **1950**, *9*.
- 48 (26) Srivastava, S.; Ruane, P. H.; Toscano, J. P.; Sullivan, M. B.; Cramer, C. J.; Chiapperino, D.; Reed,  
49 E. C.; Falvey, D. E. Structures of Reactive Nitrenium Ions: Time-Resolved Infrared Laser Flash  
50 Photolysis and Computational Studies of Substituted N-Methyl-N-arylnitrenium Ions. *Journal of the*  
51 *American Chemical Society* **2000**, *122* (34), 8271-8278.
- 52 (27) Davidse, P. A.; Kahley, M. J.; McClelland, R. A.; Novak, M. Flash Photolysis Observation and  
53 Lifetimes of 2-Fluorenyl- and 4-Biphenylacetylnitrenium Ions in Aqueous Solution. *Journal of the*  
54 *American Chemical Society* **1994**, *116* (10), 4513-4514.

- 1 (28) Wright, B. B.; Platz, M. S. Electron spin resonance spectroscopy of the triplet state of m-xylylene.  
2 *Journal of the American Chemical Society* **1983**, *105* (3), 628-630.
- 3 (29) Haider, K.; Soundararajan, N.; Shaffer, M.; Platz, M. S. EPR spectroscopy of a diaza derivative of  
4 meta-xylylene. *Tetrahedron Letters* **1989**, *30* (10), 1225-1228.
- 5 (30) Rajca, A.; Shiraishi, K.; Pink, M.; Rajca, S. Triplet (S = 1) Ground State Aminyl Diradical. *Journal*  
6 *of the American Chemical Society* **2007**, *129* (23), 7232-7233.
- 7 (31) Zhang, H.; Pink, M.; Wang, Y.; Rajca, S.; Rajca, A. High-Spin S = 3/2 Ground-State Aminyl  
8 Triradicals: Toward High-Spin Oligo-Aza Nanographenes. *Journal of the American Chemical Society*  
9 **2022**, *144* (42), 19576-19591.
- 10 (32) Arikawa, S.; Shimizu, A.; Shiomi, D.; Sato, K.; Takui, T.; Sotome, H.; Miyasaka, H.; Murai, M.;  
11 Yamaguchi, S.; Shintani, R. A Kinetically Stabilized Nitrogen-Doped Triangulene Cation: Stable and  
12 NIR Fluorescent Diradical Cation with Triplet Ground State. *Angewandte Chemie International Edition*  
13 **2023**, *62* (29).
- 14 (33) Ganley, J. M.; Murray, P. R. D.; Knowles, R. R. Photocatalytic Generation of Aminium Radical  
15 Cations for C–N Bond Formation. *ACS Catalysis* **2020**, *10* (20), 11712-11738.
- 16 (34) Su, Z.; Mariano, P. S.; Falvey, D. E.; Yoon, U. C.; Oh, S. W. Dynamics of Anilinium Radical  $\alpha$ -  
17 Heterolytic Fragmentation Processes. Electrofugal Group, Substituent, and Medium Effects on  
18 Desilylation, Decarboxylation, and Retro-Aldol Cleavage Pathways. *Journal of the American Chemical*  
19 *Society* **1998**, *120* (41), 10676-10686.
- 20 (35) Pratley, C.; Fenner, S.; Murphy, J. A. Nitrogen-Centered Radicals in Functionalization of sp<sup>2</sup>  
21 Systems: Generation, Reactivity, and Applications in Synthesis. *Chemical Reviews* **2022**, *122* (9), 8181-  
22 8260.

23